JOURNAL OF BACTERIOLOGY, Nov. 1994, p. 6653–6662
0021-9193/94/$04.00+0

Vol. 176, No. 21

Use of Transposon Tn*phoA* To Identify Genes for Cell Envelope Proteins of *Escherichia coli* Required for Long-Chain Fatty Acid Transport: the Periplasmic Protein Tsp Potentiates Long-Chain Fatty Acid Transport

AZLIYATI AZIZAN AND PAUL N. BLACK*

Department of Biochemistry, College of Medicine, The University of Tennessee, Memphis, Tennessee 38163

Received 23 May 1994/Accepted 29 August 1994

Tn*phoA* was used to mutagenize the chromosome in an effort to identify membrane-bound and exported components of the long-chain fatty acid transport system of *Escherichia coli*. This strategy identified three classes of fusions that were unable to grow or grew at reduced rates on minimal agar plates containing the long-chain fatty acid oleate ($C_{18:1}$), (i) *fadL-phoA*, (ii) *tolC-phoA*, and (iii) *tsp-phoA*. *fadL-phoA* and *tolC-phoA* fusions were unable to grow on oleate as the sole carbon and energy source, while the *tsp-phoA* fusion had a markedly reduced growth rate. As expected, *fadL-phoA* fusions were unable to grow on oleate plates because the outer membrane-bound fatty acid transport protein FadL was defective. The identification of multiple *fadL-phoA* fusions demonstrated that this strategy of mutagenesis specifically targeted membrane-bound and exported components required for growth on long-chain fatty acids. *tolC-phoA* fusions were sensitive to fatty acids (particularly medium chain) and thus unable to grow, whereas the reduced growth rate of *tsp-phoA* fusions on oleate was apparently due to changes in the energized state of the outer membrane or inner membrane. *tsp-phoA* fusions transported the long-chain fatty acid oleate at only 50% of wild-type levels when cells were energized with 1 mM DL-lactate. Under conditions in which transport was measured in the absence of lactate, *tsp-phoA* fusion strains and wild-type strains had the same levels of oleate transport. The *tsp*$^+$ clone pAZA500 was able to restore wild-type transport activity to the *tsp-phoA* strain under lactate-energized conditions. These results indicate that the periplasmic protein Tsp potentiates long-chain fatty acid transport.

Biological membrane transport systems are highly selective, allowing specific passage of the exogenous nutrients required for cell growth and maintenance. The cell envelope of the gram-negative bacterium *Escherichia coli* represents a formidable barrier for the uptake of these compounds; it is composed of two functionally distinct membranes that are separated by the periplasmic space. The outer membrane is asymmetric, containing an outer layer of lipopolysaccharide and an inner layer of phospholipid. The inner leaflet of the outer membrane is associated with a layer of peptidoglycan. The outer membrane layer contains specific proteins which facilitate nutrient transport and are classified into three groups on the basis of their functional properties: (i) nonspecific or general porins, (ii) specific channels, and (iii) high-affinity, energy-dependent transport systems (33, 34). The inner membrane is more typical of a phospholipid membrane and contains, in addition to proteins that facilitate nutrient transport, the enzymes for phospholipid biosynthesis and oxidative phosphorylation (9). The periplasmic space separates the two membrane layers and contains a number of proteins that have a catabolic function and are involved in nutrient uptake or required for detoxification. Because of the permeability properties of the bacterial cell envelope, the uptake of both hydrophilic and hydrophobic compounds requires specific transport systems.

The transport systems in *E. coli* for hydrophilic compounds are well characterized (34, 37). In contrast, the transport systems that govern the passage of hydrophobic compounds are less well defined. The primary focus of our work is to define the components and the mechanism that govern the transport of long-chain fatty acids (C_{12} to C_{18}) across the *E. coli* cell envelope. This process minimally requires the outer membrane fatty acid binding and transport protein FadL and the inner membrane-associated acyl coenzyme A (acyl-CoA) synthetase. Both of these proteins have been purified and characterized, and their respective genes (*fadL* and *fadD*, respectively) have been cloned and sequenced (2–7, 16, 17, 21, 22). FadL binds exogenous long-chain fatty acids with a relatively high affinity ($K_d = 2 \times 10^{-7}$ M oleate) and by an undefined mechanism transports these compounds across the outer membrane (2). Therefore, FadL has substrate affinity that is intermediate between the specific channels and the high-affinity, energy-dependent transport systems of the outer membrane. Acyl-CoA synthetase activates long-chain fatty acids concomitant with transport across the inner membrane by a process that proceeds through the pyrophosphorolysis of ATP (12, 19). The mechanisms that govern the passage of these compounds across the periplasmic space and the inner membrane are undefined. An oleic acid binding protein postulated to be a H^+-fatty acid cotransporter in the inner membrane has been purified and partially characterized, although this is controversial (15, 18, 25). The structural gene encoding this inner membrane protein has not been identified.

On the basis of well-characterized bacterial transport systems, we postulated that in addition to FadL and acyl-CoA synthetase, there may be other components of the long-chain fatty acid transport system. In particular, we suspected that a

* Corresponding author. Mailing address: Department of Biochemistry, College of Medicine, The University of Tennessee, 858 Madison Ave., Memphis, TN 38163. Phone: (901) 448-6576. Fax: (901) 448-7360.

periplasmic binding protein and an inner membrane permease, i.e., H^+-fatty acid cotransporter, may be required for the specific transport of long-chain fatty acids. The key to identifying these additional proteins required the generation and characterization of mutants defective in long-chain fatty acid transport. The identification and characterization of such mutants would facilitate the isolation of structural genes that encode these additional transport components for more thorough analyses.

The use of the transposon Tn*phoA* for random mutagenesis is useful in that specific mutants that contain a fusion between alkaline phosphatase (product of *phoA*) and the protein product of a target gene that is either exported or membrane bound can be selected (13, 27, 28). Therefore, we reasoned that Tn*phoA* would be a useful tool in identifying additional genes associated with the long-chain fatty acid transport apparatus. Tn*phoA* inserts randomly into a target gene, thereby generating a fusion to alkaline phosphatase. If the target gene product is either membrane bound or exported, active alkaline phosphatase fusions that are capable of being detected with the chromogenic substrate 5-bromo-4-chloro-3-indolyl-phosphate (XP; colonies appear blue) can be generated. Active *phoA* fusions unable to grow on the long-chain fatty acid oleate ($C_{18:1}$) could be screened from the population of blue colonies following λ Tn*phoA* infection of an *E. coli* strain containing a Δ*phoA* mutation, thereby facilitating the identification of additional genes required for long-chain fatty acid transport. In this study, in addition to *fadL* fusions, we identified *phoA* fusions to *tolC* and *tsp* that were either unable to grow or grew at reduced rates on minimal oleate agar plates. Fusions to *tolC* appear to affect membrane stability while fusions to *tsp* affect long-chain fatty acid transport. From these studies, we postulate that the periplasmic protein Tsp is involved in the energetics of long-chain fatty acid transport.

MATERIALS AND METHODS

Bacterial strains, plasmids, bacteriophages, and growth conditions. The bacterial strains used in these studies are listed in Table 1. Bacterial cultures were grown at 37°C in a Lab Line gyratory shaker in Luria broth (LB) or tryptone broth (TB). When minimal medium was required, medium E or medium M9 supplemented with vitamin B_1 was used (30). Carbon sources, sterilized separately, were added to final concentrations of 25 mM glucose, potassium acetate, or succinate or 5 mM decanoate or oleate. When oleate or decanoate was used as the carbon source, polyoxyethylene 20 cetyl ether (Brij 58) was added to a final concentration of 0.5%. As required, amino acids were added to a final concentration of 0.01%. When required to maintain plasmids, antibiotics were added to the following final concentrations: 100 μg of ampicillin per ml, 10 μg of tetracycline per ml, 40 μg of chloramphenicol per ml, and 40 μg of kanamycin per ml. The growth of bacterial cultures was routinely monitored with a Klett-Summerson colorimeter equipped with a blue filter.

Generalized P1 transduction of the appropriate *phoA* fusions into the prototrophic strain K-12 and the Δ*fadR* strain RS3040 followed standard protocols (30). The details of the transduction experiments are presented below (see Results).

Generation of transposon insertions containing *phoA* fusions. For mutagenesis, we used the Δ*phoA* strain CC117 (27). Cells were grown in TB containing 10 mM $MgSO_4$ and 25 mM maltose to late log phase (~2×10^9 cells per ml) and incubated with λ Tn*phoA* at a multiplicity of infection of 1 (by using 100-μl samples) (13). Incubation was continued for 15 min at room temperature, and samples were diluted 1:10 in TB to allow outgrowth. Following outgrowth for 2 h at 30°C with aeration, 0.2-ml aliquots were plated on LB plates containing 20 μg of kanamycin per ml and 40 μg of XP (*p*-toluidine salt) per ml (LBKXP plates). Plates were incubated at 30°C for 2 to 4 days or until colonies appeared. Kanamycin was included to select for transposition (selectable marker on λ Tn*phoA*), and XP was included to select for colonies with functional alkaline phosphatase (colonies were blue). Between 1 and 1.65% of the total colonies were blue (see Table 2). Following primary selection as described, all blue, kanamycin-resistant (Kn^r) colonies were stippled to minimal media containing 5 mM oleate and incubated at 37°C. The phenotypes of the Kn^r blue colonies were monitored over a 96-h period. Bacteriophage P1 lysates were prepared on each Kn^r blue colony that was unable to grow (Ole^-) or grew at a reduced rate on minimal oleate plates (Ole^{slow}; growth observed between 72 and 96 h) and used to transduce the Δ*phoA* strain CC117. The phenotypes of the resultant transductants were evaluated, and only those that retained the Kn^r blue Ole^- and Ole^{slow} phenotypes were characterized further.

TABLE 1. *E. coli* strains used in this study

Strain	Genotype	Source
CC117	*araD139* Δ(*ara leu*)*7697* Δ*lacX74* *phoA*Δ*20* *galE galK thi rpsE rpoB argE*(Am)	Manoil and Beckwith (27)
LS1187	C600 Δ*fadR*	C. DiRusso
LS1548	Δ*fadR*	C. DiRusso
K12	Prototrophic	Lab collection
PN294	CC117 *fadL-phoA1*	This study
PN295	CC117 *fadL-phoA2*	This study
PN296	CC117 *tsp-phoA3*	This study
PN297	CC117 *tsp-phoA4*	This study
PN300	CC117 *fadL-phoA7*	This study
PN301	CC117 *tolC-phoA8*	This study
PN304	CC117 *tolC-phoA11*	This study
PN305	CC117 *tolC-phoA12*	This study
PN307	CC117 *tolC-phoA14*	This study
PN314	CC117 *fadL-phoA18*	This study
PN320	CC117 *fadL-phoA24*	This study
PN370	LS1548 *fadL-phoA1*	This study
PN469	K-12 *fadL-phoA1*	This study
PN510	K-12 *tsp-phoA3*	This study
PN511	K-12 *tolC-phoA14*	This study
PN514	LS1548 *tsp-phoA3*	This study
PN515	LS1548 *tolC-phoA14*	This study

General recombinant DNA methods. Restriction, ligation, and transformation procedures have previously been described (38). Chromosomal DNA was isolated according to the method of Marmur (29). The cloning and characterization of each *phoA* fusion are described below (see Results). Small-scale plasmid isolation was achieved by alkaline lysis (38). Large-scale isolation of plasmid DNA was accomplished with Qiagen columns as specified by the vendor. Plasmid DNA was isolated and sequenced by the chain termination method of Sanger et al. (39) with [α-^{35}S]dATP and Sequenase (version 2.0; U.S. Biochemicals). A synthetic oligonucleotide complementary to the *phoA* gene was used as a primer (5'GTGCAGTAATA TCGCCC3'; complementary to the 5' end of *phoA*) for all sequencing experiments (8). Oligonucleotides were synthesized on a Gene Assembler Plus (Pharmacia LKB). The nucleotide sequence obtained for each fusion was used to search the GenBank database with the program FASTA (Genetics Computer Group, University of Wisconsin [11]).

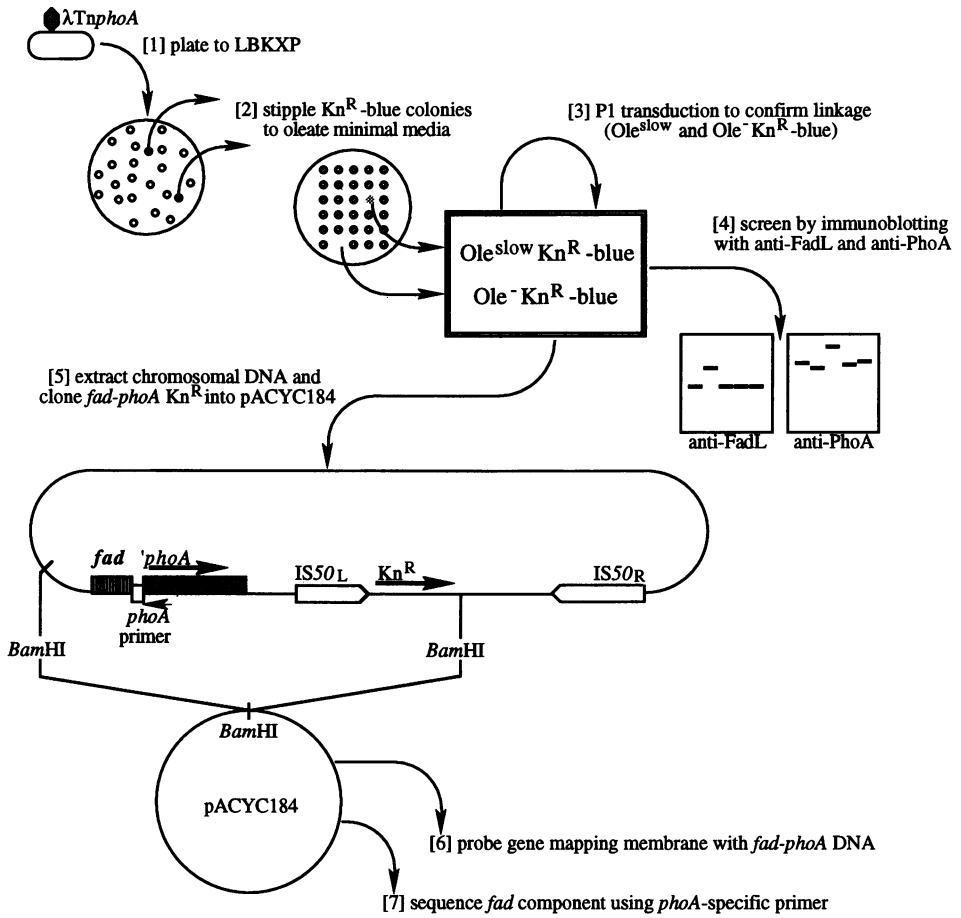

FIG. 1. Generation, screening, and identification of active *phoA* fusions that disrupt growth on the long-chain fatty acid oleate ($C_{18:1}$). (Step 1) Following infection of the Δ*phoA* strain CC117 with λ Tn*phoA*, cells were plated on LBKXP. (Step 2) All blue colonies (containing an active *phoA* fusion) were stippled to oleate minimal media. Two classes of mutants were identified: those that were unable to grow on oleate (Ole^-) and those that grew at a slow rate compared with that of the wild type (Ole^{slow}; appeared between 72 and 96 h of incubation at 37°C). (Step 3) P1 transduction was used to confirm the linkage between Ole^{slow} Kn^r blue and Ole^- Kn^r blue phenotypes. Only those transductants with the proper linkage were analyzed further. (Step 4) Active *phoA* fusions were screened by immunoblotting with anti-FadL and anti-PhoA to identify fusions to the *fadL* gene and to demonstrate PhoA-reactive fusion proteins. (Step 5) Chromosomal DNA was extracted from fusion strains, and the fragment of DNA containing the *fad-phoA* Kn^r element was cloned into pACYC184. (Step 6) *fad-phoA* DNA was nick translated with [^{32}P]dATP and used to probe the GMM representing the Kohara miniset. (Step 7) The sequence of the target gene (*fad* component) was identified with a *phoA*-specific primer.

Hybridization analysis with GMM. Following the cloning of selected *phoA* fusions, restriction analysis permitted the identification of a fragment of DNA that represented the target gene. DNA fragments containing either the target gene or *'phoA* plus the target gene were gel purified with GeneClean and nick translated with [α-^{32}P]dATP by using a commercially available kit (U.S. Biochemicals). In order to visualize each member of the Kohara miniset (20) on Gene Mapping Membranes (GMM; Takara Biochemicals), λ DNA digested with *Hin*dIII was also nick translated under the same conditions. GMM were hybridized with labeled DNA fragments essentially as described by Noda et al. (36). Briefly, GMM were prehybridized in a solution containing 5× SSC (1× SSC is 0.15 M NaCl plus 0.015 M sodium citrate), 0.5% casein, 0.1% sodium *N*-lauroyl sarcosine, and 0.02% sodium dodecyl sulfate (SDS) for 2 h at 65°C. In some instances, 100 μl of diethyl pyrocarbonate per 100 ml of prehybridization solution was added, although this did not affect the results. Following prehybridization, a ^{32}P-labeled fragment (5×10^5 dpm; ca. 25 ng of DNA) and ^{32}P-labeled λ DNA (2×10^5 dpm; ca. 5 ng of DNA) were added and incubation continued overnight at 65°C. Following hybridization, GMM were washed with 2× SSC at 65°C for 15 min, 2× SSC–0.1% SDS at 65°C for 30 min, and 0.1× SSC at 65°C for 10 min. GMM were covered with plastic wrap and exposed to Kodak XRP5 X-ray film in the presence of intensifying screens (DuPont) for appropriate periods. All hybridization experiments were done at least three times to ensure proper identification of target genes.

Transport assays. Long-chain fatty acid transport was measured as previously described (21). Briefly, following growth to mid-log phase, cells were harvested, washed once with M9 containing 0.5% Brij 58 (M9-Brij), resuspended in 0.5 volume of M9-Brij containing 100 μg of chloramphenicol per ml, and starved with aeration for 15 min at 30°C. Following starvation, 1 ml of cells was added to 1 ml of a 2× reaction mixture containing 200 μM [^{3}H]oleate (potassium salt) with or without 2 mM DL-lactate as indicated. At appropriate time points (0, 2, and 4 min), aliquots (100 μl) were rapidly pipetted onto

prewetted GN-6 filters (Gelman), washed twice with M9-Brij, air dried, and counted. Results were expressed as picomoles of oleic acid transported per minute per milligram of cell protein. In those instances when decanoate (C_{10}) transport was measured, starved cells were added to a 2× reaction mixture containing 200 μM [^{14}C]decanoate and treated as described above. All data presented represent averages of at least three independent experiments.

Proline and glutamine transport were measured as described by Berger (1a).

The values presented from transport experiments represent the means from at least three independent experiments. All transport data were subjected to analysis of variance by using StatView (Abacus Concepts, Inc.).

Immunoblot analysis. Immunoblotting of cell extracts from different *phoA* fusion strains was performed as previously described (21). These experiments served as a screen to select for fusions to the *fadL* gene and to demonstrate that a PhoA-reactive fusion could be identified. Briefly, total cellular protein (25 to 100 μg) was subjected to SDS-polyacrylamide gel electrophoresis and electrophoretically transferred onto nitrocellulose membranes (pore size, 0.45 μm) (Bio-Rad) overnight at room temperature. Following transfer, membranes were pretreated for 1 h with 10% calf serum in Tris-buffered saline and then incubated with anti-FadL (1:4,000 dilution) or anti-PhoA (1:2,500 dilution) for 1 h. Membranes were washed thoroughly with Tris-buffered saline and subsequently incubated with goat anti-rabbit immunoglobulin G horseradish peroxidase conjugate (1:5,000 dilution) for 1 h. Blots were washed and developed by the addition of the peroxidase substrate diaminobenzidine (50 μg/ml) as specified by the vendor (Bio-Rad).

Chemicals. [^{3}H]oleic acid, [^{3}H]proline, [^{3}H]glutamine, [α-^{35}S]dATP, and [^{32}P]dATP were purchased from New England Nuclear. [^{14}C]decanoic acid was obtained from Sigma. Enzymes for DNA sequencing (Sequenase) were obtained from U.S. Biochemicals, and enzymes for routine DNA manipulations were obtained from Bethesda Research Laboratories, Pharmacia LKB, U.S. Biochemicals, or New England Biolabs. Goat anti-rabbit immunoglobulin G peroxidase conjugate was obtained from Bio-Rad, and anti-PhoA was obtained from Five Prime. Antibiotics and other supplements for bacterial growth were obtained from Difco and Sigma. All other chemicals were obtained from standard suppliers and were of reagent grade.

RESULTS

Generation and screening of *phoA* fusions resulting in altered growth rates on oleate minimal media. Figure 1 illustrates the regimen used to generate, screen, and identify genes predicted to be involved in long-chain fatty acid transport. The Δ*phoA* strain CC117 was infected with λ Tn*phoA*, and following a period of outgrowth, cells were plated on LBKXP. Approximately 1.2% of the Kn^r colonies selected contained an active fusion and were stippled to minimal media containing oleate ($C_{18:1}$), decanoate (C_{10}), acetate, and dextrose. Of these active fusions, approximately 1% were unable to grow or grew at reduced rates on oleate minimal media (Ole$^-$ and Ole^{slow}, respectively; designated *fad-phoA* [Table 2]). We predicted that on oleate minimal plates either of these phenotypes could arise from transposition into *fadL* or a novel gene encoding a membrane-bound or exported protein (e.g., periplasmic and/or inner membrane) involved in long-chain fatty acid transport. Forty *fad-phoA* mutants were screened for the presence of wild-type FadL by immunoblotting of total cellular protein and polyclonal anti-FadL. Of the 40 *fad-phoA* mutants selected as described above, 18 either did not contain FadL or contained a FadL-reactive fusion protein and thus were presumed to represent *fadL-phoA* fusions. The remaining *fad-phoA* mutants were presumed to contain a fusion to a novel gene encoding a periplasmic or membrane-bound protein involved in long-chain fatty acid transport. Figure 2 is a representative immunoblot of one *fadL* fusion strain and two independent fusion strains.

TABLE 2. Generation and primary screening of *fad-phoA* fusions in the Δ*phoA* strain CC117

Experiment	No. of colonies		% Active *phoA* fusions	No. Kn^r blue Ole^{slow} or Ole$^-$ (*fad-phoA*)[a]	% Active fusions Ole^{slow} or Ole$^-$ (*fad-phoA*)
	Kn^r	Kn^r blue			
1	146,020	1,626	1.11	9	0.0062
2	41,700	481	1.15	7	0.0167
3	43,680	718	1.65	6	0.0137
4	31,750	320	1.01	6	0.0189
5	40,560	498	1.23	8	0.0197
6	28,770	316	1.08	4	0.0139
Total	332,480	3,959	1.19	40	0.0120

[a] Ole^{slow} indicates growth observed on minimal oleate plates between 72 and 96 h of incubation at 37°C; Ole$^-$ indicates no growth observed on oleate minimal plates after 96 h.

Generalized P1 transduction was employed to ensure that the phenotype defined for each *fad-phoA* fusion was the result of a single transposition event. Of the 27 *fad-phoA* strains tested (5 presumed to represent *fadL-phoA* fusions and 22 presumed to represent novel *fad-phoA* fusions), 22 P1 phage stocks prepared from this collection were able to confer an altered phenotype on strains grown on oleate plates following transduction. Eleven of these transductants also had either no growth or decreased growth rates on minimal agar plates containing either glucose, acetate, or succinate as the sole carbon and energy source. Given that these fusions may be in genes involved in amino acid uptake, oxidative phosphorylation, or the tricarboxylic acid cycle, they were not considered further. Of the 11 remaining *phoA* fusions, 5 were presumed to be in the *fadL* gene from the immunoblotting data and 6 were presumed to represent novel *fad-phoA* fusions. These six were split into two categories on the basis of growth rates on oleate, Ole$^-$ and Ole^{slow}. The identities of the five *fadL-phoA* fusions were confirmed by complementation of the Ole$^-$ phenotype following transformation with the *fadL*$^+$ clone pN130 (3).

Cloning the *fad-phoA* insertions and identification of the target gene. Three *phoA* fusion strains (one from each class)

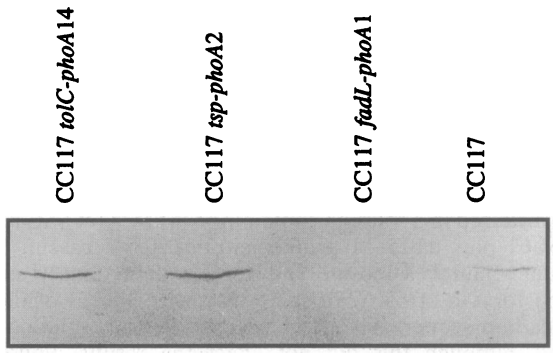

FIG. 2. Immunoblot of selected fusions probed with anti-FadL.

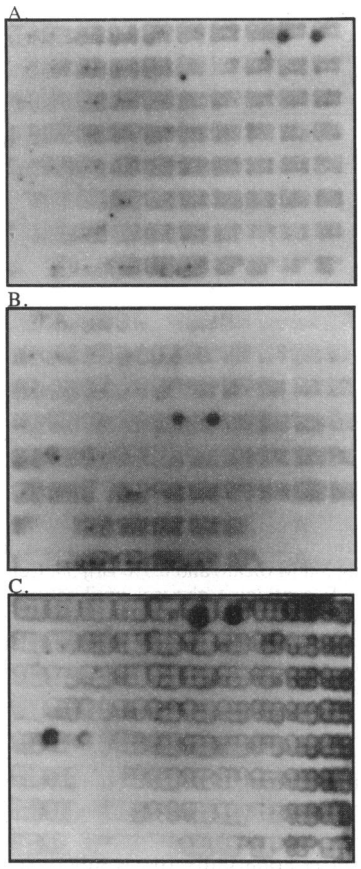

FIG. 3. GMM demonstrating hybridization of *fad*-specific DNA from pAZA294 to clones 409 and 410 (*fadL*) (A), *fad-phoA*-specific DNA from pAZA296 to clones 335 and 336 (*tsp*) (B), and *fad-phoA*-specific DNA from pAZA301 to clones 506 and 507 (*tolC*) (C). Note that the *phoA* gene gives a positive signal (clones 142 and 143) in panels B and C.

were chosen to define the target gene: PN294 (Ole$^-$; *fadL-phoA1* fusion), PN296 (Ole^{slow}; target gene unknown), and PN301 (Ole$^-$; target gene unknown). Chromosomal DNA was isolated from each strain and digested with *Bam*HI, and fragments were cloned into pACYC184. As noted in Fig. 1, there is a single *Bam*HI site downstream from the Kn^r gene of Tn*5*. We reasoned that a *Bam*HI fragment would therefore contain the entire Kn^r gene, *'phoA*, and part of the target gene. Ligation mixtures containing chromosomal DNA from each strain were transformed into the Δ*fadR* strain LS1187, and transformants were selected on LBKXP plates. As expected, blue Kn^r colonies were selected. Plasmids (designated pAZA 294, pAZA296, and pAZA301 from these three strains, respectively) were extracted from Kn^r blue colonies and shown to contain *'phoA* and the Kn^r gene from the Tn*phoA* element by restriction mapping. The approximate positions of the target genes were also identified by restriction mapping. DNA fragments containing either the target gene or the target gene and the *'phoA* gene were isolated, nick translated, and used to probe a GMM (Fig. 3). As expected, the target gene insert (*fadL*) from strain PN294 hybridized with Kohara clones 409 and 410 (representing the 50-min region of the *E. coli* chromosome; see reference 36 for the patterns of clones). The map positions for PN296 and PN301 were 40 and 66 min, respectively, on the *E. coli* chromosome. In the case of the *phoA* fusion strains PN296 and PN301, *'phoA* linked to the target gene was also nick translated and used to probe the GMM. This served as an internal control and demonstrated that *phoA* hybridized to clones 142 and 143 (which map to 8.9 min on the *E. coli* chromosome).

TABLE 3. Classification of *fad-phoA* mutants[a]

Fusion and strain	Fusion plasmid[b]	Positive Kohara clones[c]	Map position (min)[d]	Plasmid[e]
fadL-phoA				
PN294	pAZA294	409, 410	50	pN130
PN295				
PN300				
PN314				
PN320				
tsp-phoA				
PN296	pAZA296	335, 336	40	pAZA500
PN297	pAZA297			
tolC-phoA				
PN301	pAZA301	506, 507	66	pAZA200
PN304	pAZA304			
PN305				
PN307	pAZA307			

[a] Based on the identity of the target gene of each fusion from sequencing and immunoblots with polyclonal anti-FadL.
[b] Each plasmid designated contains the active *phoA* fusion linked to the Kn^r gene isolated from chromosomal DNA prepared from the identified fusion strain.
[c] Positive clones from the Kohara library following hybridization of the *fad-phoA* insert to GMM.
[d] Determined from GMM of the ordered set of λ genomic clones from the Kohara library.
[e] Plasmid clone that restores either the Ole^{slow} defect or Ole$^-$ defect (see text for details).

The DNA sequence of each target gene in plasmids pAZA 294, pAZA296, and pAZA301 was defined by dideoxy sequencing with a *phoA*-specific primer (Fig. 1). The nucleotide sequences of target genes were used to search the GenBank database. As expected, the target gene sequence obtained from pAZA294 was identical to the *fadL* sequence. The target genes in pAZA296 and pAZA301 were the *tsp* (*prc*) and the *tolC* genes, respectively (14, 35, 41). Two additional *tolC-phoA* fusions (in plasmids pAZA304 and pAZA307) hybridized to the same Kohara clones as did pAZA301. The second *tsp-phoA* fusion (in plasmid pAZA297) gave the same hybridization results as did pAZA296 (data not shown). Table 3 summarizes the data, including the identities of the target genes, from these analyses of mutants selected with Tn*phoA*.

Complementation experiments with clones of *fadL* (pN130), *tsp* (pAZA500), and *tolC* (pAZA200). All *fadL-phoA* fusions were complemented by the *fadL*$^+$ clone pN130. We obtained the *tsp*$^+$ clone pKS6-1w from R. Sauer (Massachusetts Institute of Technology) and subcloned the *Eco*RI fragment containing the *tsp* gene into pACYC184 to generate pAZA500. We chose to use pACYC184 because it has a low copy number and thus is more ideally suited as a vector for these studies. pAZA500 was able to complement the Ole^{slow} defect observed in *tsp-phoA* strains PN296, PN297, PN510, and PN514. The *tolC* gene was cloned from an *E. coli* genomic library in cosmid pLFR1 (obtained from D. Ohman) as previously described (35) into pACYC177 to generate pAZA200. This clone was able to complement the Ole$^-$ defect in PN301, PN304, and PN305 and the Dec$^-$ defect in PN515 (see below) (Table 3).

Characterization of *fadL-phoA*, *tolC-phoA*, and *tsp-phoA* mutations in the prototrophic strain K-12 and the Δ*fadR* strain

TABLE 4. Characteristics of *fadL-phoA*, *tsp-phoA*, and *tolC-phoA* mutations in wild-type (K-12) and Δ*fadR* backgrounds

Strain	Relevant genotype	Phenotype[a]		
		Oleate	Decanoate	Acetate
K-12	Wild type	+	−	+
LS1548	Δ*fadR*	+	+	+
PN469	*fadL-phoA1*	−	−	+
PN370	Δ*fadR fadL-phoA1*	−	+	+
PN510	*tsp-phoA3*	Slow	−	+
PN514	Δ*fadR tsp-phoA3*	Slow	Slow	+
PN511	*tolC-phoA14*	Slow	−	+
PN515	Δ*fadR tolC-phoA14*	Slow	−	+

[a] +, growth observed between 24 and 48 h at 37°C on the indicated minimal agar plate; Slow, growth observed between 48 and 72 h at 37°C; −, no growth observed at 96 h and 37°C.

LS1548. Given the data generated above, we were interested in defining the characteristics of each of these insertion mutations in wild-type and Δ*fadR* backgrounds. Bacteriophage P1 lysates prepared on the original isolates and shown to carry the Kn^r blue Ole^- and Ole^{slow} phenotypes associated with each of these fusions were used to transduce the prototrophic strain K-12 and the Δ*fadR* strain LS1548. The strain designations and phenotypic characteristics of these transductants are given in Table 4. Surprisingly, only the *fadL-phoA* fusion strain resulted in an Ole^- phenotype. *tsp-phoA* and *tolC-phoA* fusions resulted in Ole^{slow} phenotypes. Of initial interest, however, was the phenotype of the *tolC-phoA* transductant in the Δ*fadR* strain on decanoate minimal medium. This fusion strain (unlike the parent) was unable to grow on decanoate (Dec^-) and, therefore, indicated to us that *tolC* may be involved in medium-chain fatty acid uptake. This was not the case, however; we demonstrated that this phenotype was the result of decanoate toxicity (Table 5). Furthermore, these fusion strains had wild-type levels of long-chain fatty acid transport when not exposed to medium- or long-chain fatty acids during growth (Table 5). Given that defects in the *tolC* gene have previously been shown to result in detergent sensitivity (31), we believed that the *phoA* fusions in *tolC* were selected because of detergent or fatty acid sensitivity. The addition of 0.5% Brij 58 to TB did not affect the growth of the *tolC-phoA* fusion strain (Table 5). This was in contrast to TB containing 5 mM decanoate or oleate (in addition to 0.5% Brij 58). In these cases, growth was either abolished or slowed, respectively. This indicates that *tolC* fusions result in fatty acid (but not Brij 58) sensitivity. The *tsp-phoA* fusion strains were reproducibly Ole^{slow}. When the growth kinetics of Δ*fadR tsp-phoA3* and *tsp-phoA3* strains on oleate liquid minimal media were compared with those of Δ*fadR* and wild-type strains, a distinct lag in strains containing the *tsp-phoA3* fusion was apparent (Fig. 4). The lag in the *tsp-phoA3* fusion is apparently the result of a null mutation since the insertion is at amino acid 37 of the wild-type gene (data not shown). The lag in growth was also present in cells pregrown in acetate or succinate, indicating that the prior carbon source does not influence this process.

TABLE 5. Fatty acid transport in *tolC-phoA* and *fadL-phoA* fusion strains

Strain	Genotype	Fatty acid transport (pmol/min/mg)[a]		Growth[b]		
		$C_{18:1}$	C_{10}	TBDec	TBOle	TBBrij
LS1548	Δ*fadR*	903	861	+	+	+
PN515	Δ*fadR tolC-phoA14*	1,099	1,053	−	Slow	+
PN370	Δ*fadR fadL-phoA1*	12	Not tested	+	+	+

[a] Picomoles of fatty acid transported per minute per milligram of protein following growth in TB as described in Materials and Methods.

[b] TBDec, TB containing 5 mM decanoate and 0.5% Brij 58; TBOle, TB containing 5 mM oleate and 0.5% Brij 58; TBBrij, TB containing 0.5% Brij 58. Growth as noted in footnote *a* of Table 4.

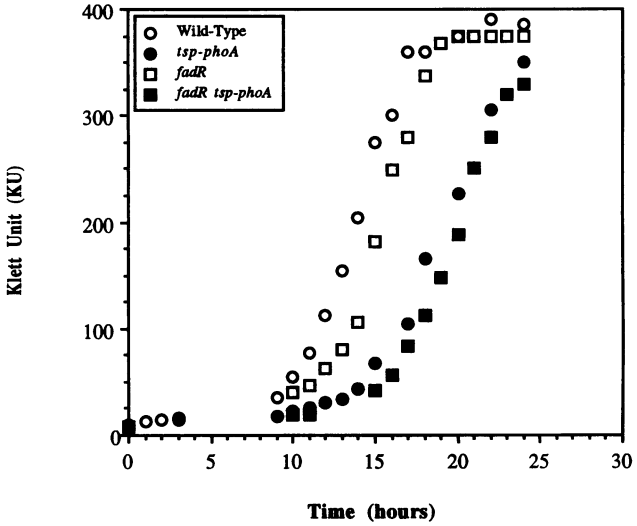

FIG. 4. Growth curves of *tsp-phoA* fusion strains in minimal medium E containing 5 mM oleate and 0.5% Brij 58. Cells were grown in minimal medium E containing glycerol until saturation, pelleted by centrifugation, washed with medium E, and resuspended in the original volume of medium E. Cultures were inoculated to an initial Klett unit level of 5 to 10 (2.5×10^7 to 5.0×10^7 cells per ml), and growth at 37°C was monitored as indicated.

Contribution of Tsp to long-chain fatty acid transport. As noted above, wild-type and Δ*fadR* transductants containing the *tsp-phoA3* fusion had a significant lag period when grown in oleate minimal media. We conclude that this long lag period was a contributing factor to the reduced growth rates (and thus the Ole^{slow} phenotype) of the original *tsp-phoA* isolates in the Δ*phoA* strain CC117. Given this phenotype, we were interested in determining whether the overall rates of long-chain fatty acid uptake in wild-type and Δ*fadR* strains containing the *tsp-phoA3* insertion (strains PN510 and PN514, respectively) were reduced. As noted above, *tolC-phoA* fusions did not affect long-chain fatty acid transport; thus, we concluded that they arise as a consequence of fatty acid sensitivity. All of the *fadL-phoA* fusions tested were unable to transport the long-chain fatty acid oleate (Table 5 and data not shown).

When the levels of oleate transport in Δ*fadR* and Δ*fadR tsp-phoA3* strains were measured, no apparent alterations were observed except under conditions in which cells were energized with 1 mM DL-lactate prior to transport (Fig. 5). The addition of D-lactate stimulates long-chain fatty acid transport by an undefined mechanism that is proposed to involve the partitioning of acyl-CoA synthetase in the inner membrane (26). When transport was measured in the presence of 1 mM DL-lactate, there was a significant difference in the rates of oleate transport between the Δ*fadR* and Δ*fadR tsp-phoA* strains ($P = 0.0003$; Fig. 4). While there was a slight elevation in the rate of transport in the presence of lactate for the Δ*fadR tsp-phoA3* strain, this difference was not significant ($P = 0.3125$). The tsp^+ plasmid, pAZA500 (which complemented the Ole^{slow} pheno-

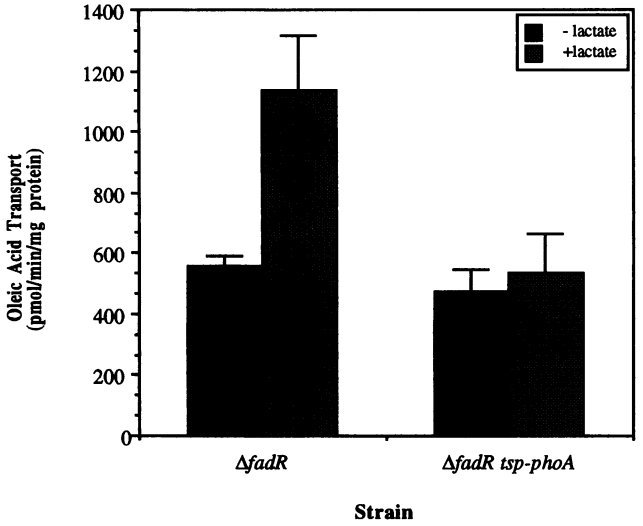

FIG. 5. Oleate transport of the Δ*fadR* strain LS1548 and the Δ*fadR tsp-phoA3* strain PN514 with (+) and without (−) 1 mM DL-lactate in the reaction mixture following growth in TB. Error bars represent the standard errors of means from five independent experiments.

type in the Δ*fadR tsp-phoA3* strain PN514; see above), was able to restore the stimulatory effect of lactate on long-chain fatty acid transport (Fig. 6).

In order to make certain that the *tsp* insertion mutation was specific for the long-chain fatty acid uptake system, we also measured proline transport (an example of a shock-resistant transport system) and glutamine transport (an example of a shock-sensitive system). The addition of 1 mM DL-lactate to assay buffers was stimulatory for both (particularly proline) transport systems, but there were no significant differences observed between Δ*fadR* and Δ*fadR tsp-phoA3* strains (Fig. 7). These data argue that Tsp was specifically involved in potentiating the rate of uptake of long-chain fatty acids. This

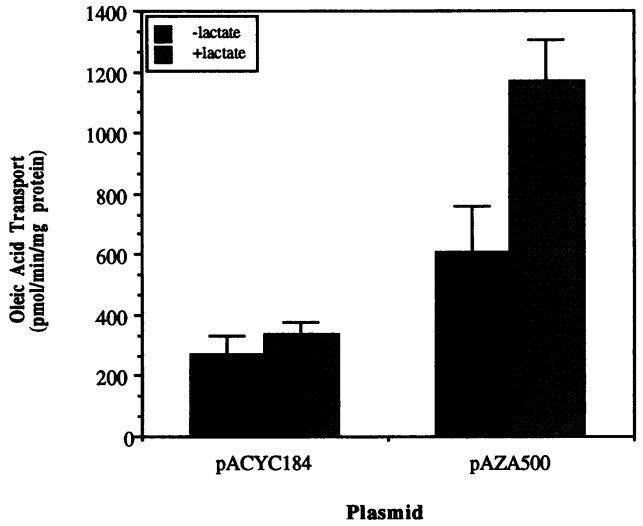

FIG. 6. Oleate transport of the Δ*fadR tsp-phoA3* strain PN514 following transformation with pACYC184 or the *tsp*$^+$ plasmid pAZA500 with (+) and without (−) 1 mM DL-lactate in the reaction mixture. Error bars represent the standard errors of means from three independent experiments.

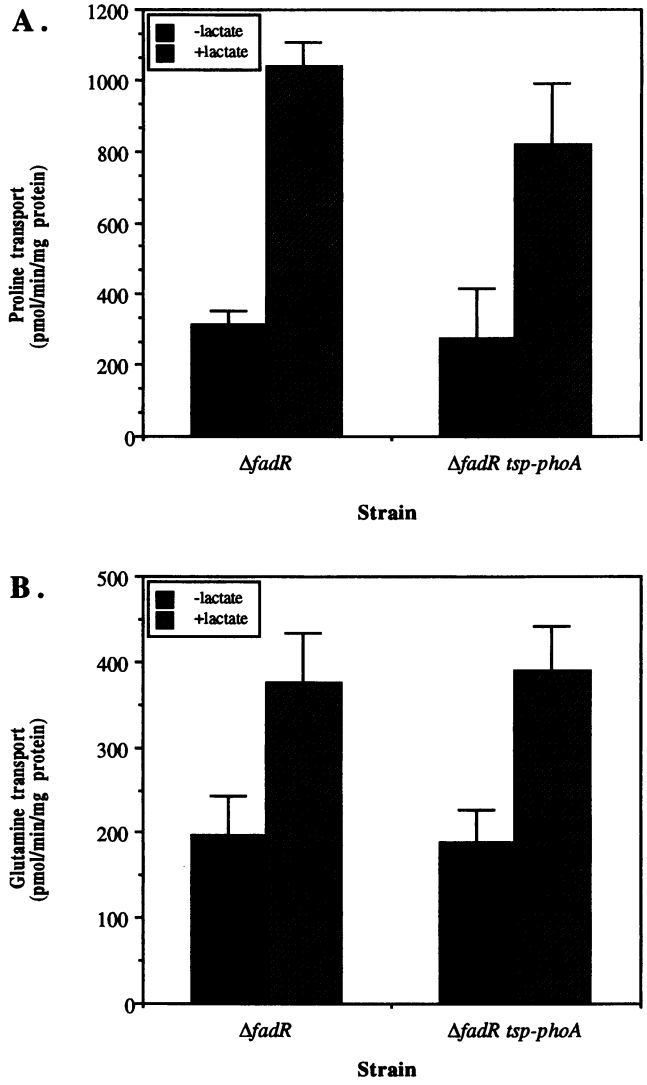

FIG. 7. Proline transport (A) and glutamine transport (B) of the Δ*fadR* strain LS1548 and the Δ*fadR tsp-phoA3* strain PN514 with (+) and without (−) 1 mM DL-lactate in the reaction mixture. Error bars represent the standard errors of means from three independent experiments.

enhancement in the presence of lactate may indicate that metabolic energy is transduced through Tsp to FadL, thereby facilitating optimal levels of long-chain fatty acid transport.

DISCUSSION

The goal of this work was to identify additional structural genes required for long-chain fatty acid transport in *E. coli*. We chose to use the transposon Tn*phoA* because active alkaline phosphatase fusion proteins that were either membrane bound or exported from the cell could be selected. Under these conditions, we selected nearly 4,000 active fusions that were subsequently screened for the ability to grow on solid oleate ($C_{18:1}$) minimal media. Following several rounds of screening, we identified 11 independent *phoA* fusions that had reduced growth rates (Ole^{slow}) or were unable to grow (Ole$^-$) on oleate minimal agar plates. The target gene for each fusion was identified by molecular cloning techniques coupled with hy-

bridization to GMM (representing the Kohara miniset) (20) and DNA sequencing with a *phoA*-specific primer. Five of these fusions were to the *fadL* gene, indicating that these methods had targeted the long-chain fatty acid transport apparatus of *E. coli*. Four of these fusions were to the *tolC* gene, and two were to the *tsp* (*prc*) gene. Strains harboring mutations in *tolC* are tolerant to colicin E1, alter the expression of several outer membrane proteins, and block hemolysin secretion (31, 42). Strains harboring mutations in *tsp* (*prc*) are unable to process penicillin-binding protein 3 (14). This strategy of mutagenesis did not identify the structural gene that would encode the postulated H^+-fatty acid cotransporter of the inner membrane identified by Kameda (15). Therefore, these results tend to agree with the conclusion made by Mangroo and Gerber (25) that the fatty acid transport system of *E. coli* does not contain an inner membrane component. It should be noted, however, that caution must be used in interpreting these negative results. A *phoA* fusion to the postulated H^+-fatty acid cotransporter structural gene may be lethal and thus not detectable by these methods.

The fusions to *tolC* were of initial interest as strains harboring the *tolC-phoA* fusion were unable to grow on oleate minimal media. When the *tolC-phoA14* fusion was transduced into wild-type and Δ*fadR* strains, it became apparent that the oleate phenotype was leaky. When the phenotype of the Δ*fadR tolC-phoA* transductant was tested on minimal media containing decanoate, only the parental strain was able to grow. We initially speculated that TolC might represent a medium-chain fatty acid transporter. Further analysis, however, indicated that this fusion was sensitive to decanoate and thus failed to grow. Furthermore, the levels of medium- and long-chain fatty acid transport measured for this strain were essentially those of the wild type. Defects in *tolC* result in increased sensitivity to hydrophobic antibiotics, dyes, and detergents (31). In addition, mutations in *tolC* alter the expression of several outer membrane proteins (32). TolC is also a component of a multidrug resistance pump (23) that may be involved in protecting cells from the toxic effects of medium-chain fatty acids (40). We have demonstrated that the level of FadL in our collection of *tolC-phoA* fusions remains unchanged, indicating that the expression of this outer membrane protein was unchanged. Therefore, we have concluded that TolC is not a central component of the fatty acid transport system. It is worth pointing out, however, that this outer membrane protein may have a peripheral role in the transport of fatty acids (especially under conditions in which there are high concentrations of fatty acids and detergents) by promoting outer membrane stability.

The *pho* fusions to *tsp* were considerably more interesting. Cells containing *tsp-phoA* fusions had reduced growth rates on oleate minimal agar plates compared with that of the wild-type strain. When the specific growth rate of the *tsp-phoA3* strain PN514 in liquid oleate minimal medium was measured, it was noted that this decreased growth rate was due to an extended lag period rather than to changes during logarithmic growth. We questioned whether the phenotype of *tsp-phoA* fusion in oleate minimal medium was due to the energized state of the cell. Therefore, long-chain fatty acid transport was measured under conditions in which cells were unenergized or energized with 1 mM DL-lactate. Previous studies have demonstrated that the inclusion of lactate in the reaction mixture results in twofold stimulation of long-chain fatty acid transport (26). Data presented in this paper demonstrated that the addition of lactate failed to stimulate oleic acid transport in our Δ*fadR tsp-phoA* fusion strains. Further experiments verified these results by demonstrating that transformants of the Δ*fadR tsp-phoA3* strain PN514 harboring the *tsp*$^+$ clone pAZA500 were able to transport oleic acid at levels comparable to those of the wild-type strain when cells were energized with lactate. Finally, experiments measuring the rates of proline transport and glutamine transport (with the addition of lactate) in Δ*fadR* and Δ*fadR tsp-phoA* strains were the same, demonstrating that the failure of lactate to stimulate long-chain fatty acid transport in these strains was specific for the *phoA* fusion to *tsp*.

Data from these experiments argue that Tsp is involved in long-chain fatty acid transport at the level of energetics. The inclusion of lactate in reaction mixtures following a starvation period appears to energize cells, thereby increasing the rate of long-chain fatty acid transport. We have observed the same degree of potentiation when glucose is added to reaction mixtures prior to transport (data not shown). Mangroo and Gerber have demonstrated that this lactate effect is due to the partitioning of acyl-CoA synthetase in the inner membrane (26). In the case of acyl-CoA synthetase, this partitioning may be the result of changes in the membrane potential and/or in the enzyme related to catalytic activity (i.e., the binding of ATP). A defect in *tsp* eliminates this lactate effect and thus indicates that Tsp is involved in the potentiation of long-chain fatty acid transport. The notion that Tsp enhances long-chain fatty acid transport is distinct from the enhancement noted following the partitioning of acyl-CoA synthetase in the inner membrane. Previous data have demonstrated that Tsp is a protease involved in C-terminal processing of proteins with nonpolar carboxyl termini, including penicillin-binding protein 3 (14, 41). It seems unlikely that Tsp is involved in the processing of acyl-CoA synthetase to facilitate membrane partitioning, since this enzyme lacks a hydrophobic carboxyl terminus and, as Hara et al. (14) have proposed, Tsp (Prc) is found in the periplasmic space. High levels of alkaline phosphatase activity in the supernatant following osmotic shock of the *tsp-phoA3* strain PN296 also argue that this protein resides in the periplasmic space (data not shown). Therefore, the role of Tsp in the potentiation of long-chain fatty acid transport must occur within the periplasmic space and be responsive to the energized state of the cell.

This work suggests that Tsp has a role at the level of energy transduction to facilitate optimal levels of long-chain fatty acid transport. The outer membrane protein FadL binds long-chain fatty acids with a relatively high affinity ($K_d = 2.0 \times 10^{-7}$ M oleate). The precise mechanism that facilitates the transport of fatty acids across the outer membrane is currently under investigation. Given that FadL binds ligands with a relatively high affinity, it stands to reason that metabolic energy may be involved in facilitating ligand release. Our data demonstrating that Tsp potentiates long-chain fatty acid transport in energized cells argue that this periplasmic protein may interact with FadL to facilitate ligand release. This observation suggests that FadL may be more analogous to the high-affinity, energy-dependent transporters of the outer membrane. Silber et al. (41) demonstrated that Tsp has sequence similarity to human and bovine interphotoreceptor retinoid-binding proteins. Interphotoreceptor retinoid-binding proteins bind hydrophobic ligands, including fatty acids (24). We speculate that Tsp may bind long-chain fatty acids following their transfer across the outer membrane via FadL.

From the experiments detailed here, we propose that Tsp, in addition to FadL and acyl-CoA synthetase, is a component of the long-chain fatty acid transport system in *E. coli*. Tsp acts to potentiate the rate of long-chain fatty acid transport under conditions in which cells are energized. Therefore, we conclude that the energized state of the cell plays a pivotal role in

long-chain fatty acid uptake. It is premature to determine whether the role of Tsp in this process is direct (and thus more analogous to that of TonB) or indirect (and thus, Tsp acts as a C-terminal protease on an undefined protein that is involved in energy transduction in the long-chain fatty acid transport system). Our preliminary data support the notion that this is a direct effect. Osmotic shock experiments reduce long-chain fatty acid transport by nearly 60%, indicating that a periplasmic component (i.e., Tsp) may be involved in this process (1).

ACKNOWLEDGMENTS

We thank Priscilla Briggett and Ryoko Kita for technical assistance during the screening of *phoA* fusions, Ron Taylor for λ Tn*phoA*, Dennis Ohman for the *E. coli* genomic library in pLFR1, and Robert Sauer for pKS6-1w.

This work was supported by grants from the American Heart Association (901063) and the National Science Foundation (DCB9104646) to P.N.B. This work was done during an Established Investigatorship (P.N.B.) from the American Heart Association.

REFERENCES

1. **Azizan, A., and P. N. Black.** Unpublished data.
1a. **Berger, E. A.** 1973. Different mechanisms of energy coupling for the active transport of proline and glutamine in Escherichia coli. Proc. Natl. Acad. Sci. USA **70:**1514–1518.
2. **Black, P. N.** 1990. Characterization of FadL-specific fatty acid binding in *Escherichia coli*. Biochim. Biophys. Acta **1046:**97–105.
3. **Black, P. N.** 1991. Primary sequence of the *Escherichia coli fadL* gene encoding an outer membrane protein required for long-chain fatty acid transport. J. Bacteriol. **173:**435–442.
4. **Black, P. N., and C. C. DiRusso.** 1994. Molecular and biochemical analyses of fatty acid transport, metabolism, and gene regulation in *Escherichia coli*. Biochim. Biophys. Acta **1210:** 123–145.
5. **Black, P. N., C. C. DiRusso, A. K. Metzger, and T. L. Heimert.** 1992. Cloning, sequencing, and expression of the *fadD* gene of *Escherichia coli* encoding acyl coenzymeA synthetase. J. Biol. Chem. **267:**25513–25520.
6. **Black, P. N., S. K. Kianian, C. C. DiRusso, and W. D. Nunn.** 1985. Long-chain fatty acid transport in *Escherichia coli*. Cloning, mapping, and expression of the *fadL* gene. J. Biol. Chem. **260:**1780–1789.
7. **Black, P. N., B. Said, C. R. Ghosn, J. V. Beach, and W. D. Nunn.** 1987. Purification and characterization of an outer membrane-bound protein involved in long-chain fatty acid transport in *Escherichia coli*. J. Biol. Chem. **262:**1412–1419.
8. **Chang, C. N., W.-J. Kuang, and E. Y. Chen.** 1986. Nucleotide sequence of the alkaline phosphatase gene of *Escherichia coli*. Gene **44:**121–125.
9. **Cronan, J. E., Jr., R. B. Gennis, and S. R. Maloy.** 1987. Cytoplasmic membrane, p. 31–55. *In* F. C. Neidhardt, J. L. Ingraham, K. B. Low, B. Magasanik, M. Schaechter, and H. E. Umbarger (ed.), *Escherichia coli* and *Salmonella typhimurium*: cellular and molecular biology. American Society for Microbiology, Washington, D.C.
10. **de Bruijn, F. J., and J. R. Lupski.** 1984. The use of transposon Tn*5* mutagenesis in the rapid generation of correlated physical and genetic maps of DNA segments cloned into multicopy plasmids—a review. Gene **27:**131–149.
11. **Devereaux, J., P. Haeberli, and O. Smithies.** 1984. A comprehensive set of sequence analysis programs for the VAX. Nucleic Acids Res. **12:**387–395.
12. **Groot, P. H. E., H. R. Scholte, and W. C. Hulsmann.** 1976. Fatty acid activation: specificity, localization and function. Adv. Lipid Res. **14:**75–126.
13. **Gutierrez, C., J. Barondess, C. Manoil, and J. Beckwith.** 1987. The use of transposon Tn*phoA* to detect genes for cell envelope proteins subject to a common regulatory stimulus. J. Mol. Biol. **195:**289–297.
14. **Hara, H., Y. Yamamoto, A. Higashitani, H. Suzuki, and Y. Nishimura.** 1991. Cloning, mapping, and characterization of the *Escherichia coli prc* gene, which is involved in C-terminal processing of penicillin-binding protein 3. J. Bacteriol. **173:**4799–4813.
15. **Kameda, K.** 1986. Partial purification and characterization of fatty acid binding protein(s) in *Escherichia coli* membranes and reconstitution of fatty acid transport system. Biochem. Int. **13:**343–350.
16. **Kameda, K., and W. D. Nunn.** 1981. Purification and characterization of acyl CoA synthetase from *Escherichia coli*. J. Biol. Chem. **256:**5702–5707.
17. **Kameda, K., L. K. Suzuki, and Y. Imai.** 1985. Further purification, characterization and salt activation of acyl CoA synthetase of *Escherichia coli*. Biochim. Biophys. Acta **840:**29–36.
18. **Kameda, K., L. K. Suzuki, and Y. Imai.** 1987. Transport of fatty acid is obligatory coupled with H^+ entry in spheroplasts of *Escherichia coli* K12. Biochem. Int. **14:**227–234.
19. **Klein, K. R., R. Steinberg, B. Fiethen, and P. Overath.** 1971. Fatty acid degradation in *Escherichia coli*: an inducible system for the uptake of fatty acids and further characterization of old mutants. Eur. J. Biochem. **19:**442–450.
20. **Kohara, Y., K. Akiyama, and K. Isono.** 1987. The physical map of the whole *E. coli* chromosome: application of a new strategy for rapid analysis and sorting of a large genomic library. Cell **50:**495–508.
21. **Kumar, G. B., and P. N. Black.** 1991. Linker mutagenesis of a bacterial fatty acid transport protein. Identification of domains with functional importance. J. Biol. Chem. **206:**1348–1353.
22. **Kumar, G. B., and P. N. Black.** 1993. Bacterial long-chain fatty acid transport. Identification of amino acid residues within the outer membrane protein FadL required for activity. J. Biol. Chem. **268:**15469–15476.
23. **Lewis, K.** 1994. Multidrug resistance in bacteria: variations on a theme. Trends Biochem. Sci. **19:**119–123.
24. **Liou, G. I., L. Geng, and W. Baehr.** 1991. Interphotoreceptor retinoid-binding protein: biochemistry and molecular biology. Prog. Clin. Biol. Res. **362:**115–137.
25. **Mangroo, D., and G. E. Gerber.** 1992. Photoaffinity labeling of fatty-acid binding proteins involved in long-chain fatty acid transport in *Escherichia coli*. J. Biol. Chem. **267:**17095–17101.
26. **Mangroo, D., and G. E. Gerber.** 1993. Fatty acid uptake in *Escherichia coli*: regulation by recruitment of fatty acyl CoA synthetase to the plasma membrane. Biochem. Cell Biol. **71:**51–56.
27. **Manoil, C., and J. Beckwith.** 1985. Tn*phoA*: a transposon probe for protein export signals. Proc. Natl. Acad. Sci. USA **82:**8129–8133.
28. **Manoil, C., J. J. Mekalanos, and J. Beckwith.** 1990. Alkaline phosphatase fusions: sensors of subcellular location. J. Bacteriol. **172:**515–518.
29. **Marmur, J.** 1961. A procedure for the isolation of DNA from microorganisms. J. Mol. Biol. **3:**208–218.
30. **Miller, J. H.** 1972. Experiments in molecular genetics, p. 433–440. Cold Spring Harbor Laboratory, Cold Spring Harbor, N.Y.
31. **Morona, R., P. A. Manning, and P. Reeves.** 1983. Identification and characterization of the TolC protein, an outer membrane protein from *Escherichia coli*. J. Bacteriol. **153:**693–699.
32. **Morona, R., and P. Reeves.** 1982. The *tolC* locus of *Escherichia coli* affects the expression of three major outer membrane proteins. J. Bacteriol. **150:**1016–1023.
33. **Nikaido, H.** 1992. Porins and specific channels of bacterial outer membranes. Mol. Microbiol. **6:**435–442.
34. **Nikaido, H., and M. H. Saier, Jr.** 1992. Transport proteins in bacteria: common themes in their design. Science **258:**926–942.
35. **Niki, H., R. Imamura, T. Ogura, and S. Hiraga.** 1990. Nucleotide sequence of the *tolC* gene of *Escherichia coli*. Nucleic Acids Res. **18:**5547.
36. **Noda, A., J. B. Courtright, P. F. Denor, G. Webb, Y. Kohara, and A. Ishima.** 1991. Rapid identification of specific genes in *E. coli* by hybridization to membranes containing the ordered set of phage clones. BioTechniques **10:**414–477.
37. **Saier, M. H., Jr.** 1985. Mechanisms and regulation of carbohydrate transport in bacteria. Academic Press, Inc., New York.
38. **Sambrook, J., E. F. Fritsch, and T. Maniatis.** 1989. Molecular cloning: a laboratory manual, 2nd ed. Cold Spring Harbor Laboratory, Cold Spring Harbor, N.Y.

39. **Sanger, F., S. Nicklen, and A. R. Coulson.** 1977. DNA sequencing with chain-terminating inhibitors. Proc. Natl. Acad. Sci. USA **74:** 5463–5467.
40. **Sheu, C. W., and E. Freese.** 1973. Lipopolysaccharide layer protection of gram-negative bacteria against inhibition by long-chain fatty acids. J. Bacteriol. **115:**869–875.
41. **Silber, K. R., K. C. Keiler, and R. T. Sauer.** 1992. Tsp: a tail-specific protease that selectively degrades proteins with non-polar C termini. Proc. Natl. Acad. Sci. USA **89:**295–299.
42. **Wandersman, C., and P. Delepelaire.** 1990. TolC, an *Escherichia coli* outer membrane protein required for hemolysin secretion. Proc. Natl. Acad. Sci. USA **87:**4776–4780.